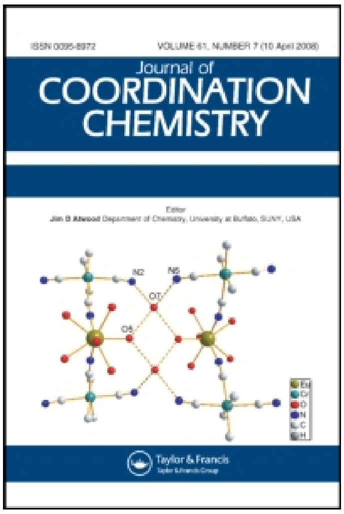

Journal of Coordination Chemistry
Publication details, including instructions for authors and subscription information:
http://www.informaworld.com/smpp/title~content=t713455674

H-OXO HETEROBINUCLEAR COMPLEXES OBTAINED BY DONOR ACCEPTOR REACTIONS WITH THE VANADYL GROUP

Chiou-Herr Yang[a]; Judith A. Ladd[a]; Virgil L. Goedken[a]
[a] Department of Chemistry, Florida State University, Tallahassee, Florida, U.S.A.

To cite this Article Yang, Chiou-Herr , Ladd, Judith A. and Goedken, Virgil L.(1988) 'H-OXO HETEROBINUCLEAR COMPLEXES OBTAINED BY DONOR ACCEPTOR REACTIONS WITH THE VANADYL GROUP', Journal of Coordination Chemistry, 18: 4, 317 — 334

To link to this Article: DOI: 10.1080/00958978808080972

URL: http://dx.doi.org/10.1080/00958978808080972

J. Coord. Chem. 1988, Vol. 18. pp. 317–334
Reprints available directly from the publisher
Photocopying permitted by license only

μ-OXO HETEROBINUCLEAR COMPLEXES OBTAINED BY DONOR ACCEPTOR REACTIONS WITH THE VANADYL GROUP

CHIOU-HERR YANG, JUDITH A. LADD AND VIRGIL L. GOEDKEN*

Department of Chemistry, Florida State University, Tallahassee, Florida 32306–3006, U.S.A.

(Received December 29, 1987; in final form April 27, 1988)

The vanadyl complex $(C_{22}H_{22}N_4)VO$, prepared by the reaction of the macrocyclic ligand, $C_{22}H_{24}N_4$, with vanadyl acetate, forms adducts with Lewis acids such as triphenylboron and trimethyl silicon. All three complexes have been characterized by EPR spectroscopy and X-ray crystallographic techniques to examine the effect of adduct formation on the V=O bonding. $VO(C_{22}H_{22}N_4)$ is triclinic, $P\bar{1}$, with a = 11.150(2), b = 12.514(3), c = 8.468(2) Å, α = 101.80(2), β = 105.09(3), γ = 76.27(2)°, d(obs) = 1.37 g cm^{-3}, d(calc) = 1.381 g/cm^3. $(C_{22}H_{22}N_4)V–O–B(C_6H_5)_3$ is monoclinic $P2_1/n$, with a = 11.174(3), b = 20.208(4), c = 14.460(8) Å, β = 97.23(1)°, d(obs) = 1.34 g cm^{-3} for $Z = 4$. $[C_{22}H_{2}2N_{4})V–O–Si(CH_3)_3]B(C_6H_5)_4$ is monoclinic, $P2_1/m$, with a = 9.884(1), b = 13.669(4), c = 16.161(3) Å, β = 105.01(1)°, d(obs) = 1.28 g cm^{-3}, d(calc) = 1.263 g cm^{-3} for $Z = 4$. The V=O bond distance, 1.601(2) Å, is typical of other vanadyl complexes; adduct formation with $B(C_6H_5)_3$ leads only to a modest lengthening to 1.665(3) Å and weak B–O interaction is indicated by the rather long B–O distance of 1.571(6) Å. Interaction of the V=O bond with $Si(CH_3)_3$ to form a V–O–Si linkage leads to a substantial lengthening of the V–O distance, 1.751(3) Å, and a Si–O distance, 1.662(3) Å, only slightly longer than the corresponding Si–O ether oxygen distance, 1.631(3) Å. The structural and ESR parameters of these complexes are compared with related vanadyl complexes.

Keywords: vanadyl, macrocycle, heterobinuclear, dimer, crystal structure

INTRODUCTION

The vanadyl species, $V{=}O^{2+}$ is the "thermodynamic sink" of much vanadium(IV) chemistry. The basicity of this oxo group is low with very little tendency to protonate in acidic solution or to interact with other metal ions. The reaction chemistry of vanadyl complexes has been largely ignored because of the inertness of the $V{=}O^{2+}$ bond[1] and the unusually high energy of the $V{=}O^{2+}$ bond (about 590 kJ mol^{-1}).[2] However, under certain conditions, the $V{=}O^{2+}$ bond can be made to react. Deoxygenation of Schiff base vanadyl complexes has been accomplished using reagents that readily form strong interactions with oxygen functions. Floriani[3,4] utilized $SOCl_2$ or PCl_5 to produce dichlorovanadium(IV) chelate complexes. Callahan[5,6] synthesized a sulfovanadium(IV) species by the deoxygenation of VO(SALEN) with B_2S_3. Both Floriani[4] and Callahan[5] reported that they attempted to deoxygenate vanadyl phthalocyanine but failed. There is no reaction when VOTPP (TPP = tetraphenylporphyrin) solutions are treated with anhydrous HC.

The reaction of $V{=}O^{2+}$ with oxophilic species forming heterobinuclear compounds, bridged through the oxygen atom, is a rare occurrence. An early solution study[7] discovered that adduct formation between the vanadyl oxygen and the ruthenium atom of $[Ru(NH_3)_5H_2O]^{2+}$ occurs readily. However, the product was

---

* Author for correspondence

only characterized by IR and UV spectra; no further details of the structure of this interesting and unusual complex have been reported.

This paper describes the synthesis and characterization of new heterobinuclear complexes formed by adduct formation between the vanadyl oxygen of the macrocyclic complex $VO(C_{22}H_{22}N_4)$ with oxophilic centers. $VO(C_{22}H_{22}N_4)$ has previously been shown to have

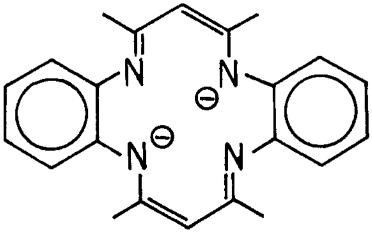

Line drawing of $C_{22}H_{22}N_4^{2-}$, the benzo[b_{ij}]-1,4,8,11-tetraazocyclotetradeca-hexaenato ligand

higher reactivity[8] than closely related vanadyl porphyrin complexes. Our choices of adducts were highly oxophilic Lewis acids such as the B atom of $B(C_6H_5)_3$ and the $Si(CH_3)_3$ anion. The successful isolation of these complexes allows us to address a number of points regarding the effect of adduct formation on the structure and bonding of the $V{=}O^{2+}$ group and provides a starting point to understand other heterobinuclear complexes. Points to be addressed in this study are how adduct formation to the V=O bond effects the strength of the V–O bond as measured by such indicators as V–O bond stretching frequency, electron spin resonance parameters of the vanadyl complexes and V–O bond distances and V–O–M angles as determined from single crystal X-ray diffraction studies.

EXPERIMENTAL

Materials and Reagents

All of the reactions described here were carried out under nitrogen atmosphere. The solvents were of reagent grade and were dried using 3A molecular sieves. The commercially obtained chemicals were used in these experiments without further purification. Infrared spectra of the solid complexes, in Nujol mulls, were recorded on a Perkin-Elmer 983 infrared spectrophotometer in the range 4000 to 250 cm^{-3}. Ultraviolet and visible spectra were obtained using a Cary 14 recording spectrophotometer within the range 20000 to 2000 Å.

Electron paramagnetic resonance spectra were recorded on a Varian E-12 spectrometer equipped with E-100 (for X-band spectra and E-110 (for Q-band spectra) microwave bridges. A Spectromagnetic Industries 5200 NMR Gausmeter was used to measure the magnetic field. The isotropic parameters were determined from X-band spectra of a 50:50 toluene:acetonitrile solution of these complexes at 20°C. The tensor components were calculated from X-band spectra measured on frozen solutions (−140°C) of the same composition.

Complex Preparation

$(C_{22}H_{22}N_4)VO$

A 15 cm^3 aliquot of anhydrous toluene was deaerated for 15 min with N_2. Then, 0.3 g of the free ligand, $C_{22}H_{22}N_4$, and 0.15 g of vanadyl acetate were added along with a drop of triethylamine. The resulting mixture was heated under reflux for 12 hrs during which time the yellow green $(C_{22}H_{22}N_4)VO$ complex precipitated from the green solution. The IR spectrum of this complex shows a new intense absorption at 965 cm^{-1} assignable to the V=O stretching frequency.

$(C_{22}H_{22}N_4)Cl_2.HCl$

0.20 g of $(C_{22}H_{22}N_4)VO$ was dissolved in 2.0 cm^3 of acetonitrile and 3 drops of concentrated HCl were added. The colour of the solution changed from green to brown as the vanadyl complex was deoxygenated. A brown crystalline precipitate began forming within minutes. After four hours, the solution was filtered, the precipitate washed with dry acetonitrile, and the product dried *in vacuo*. The IR spectrum of this dark brown solid contains no V=O stretching frequency. The presence of multiple imine bands in the region 1600–1500 cm^{-1}, together with elemental analysis suggests that the complex is protonated. The IR spectrum suggests that protonation occurs at one of the methine carbon atom positions forming the chloride salt.

$(C_{22}H_{22}N_4)V{=}O{-}B(C_6H_5)_3$; *Method A*

50 mg of $(C_{22}H_{22}N_4)VCl_2.HCl$ were suspended in a solvent mixture of 1:1 (toluene:acetonitrile) in a test tube. To this suspension, while stirring, was added 40 mg of $NaB(C_6H_5)_4$. The test tube was stoppered with a serum cap and the solution heated at 70°C for 12 hours. During this time the solution turned brown in colour and a brown precipitate formed. It is believed that the HCl adduct of the vanadyl complex liberates HCl in solution which in turn protonates the tetraphenyl borate anion producing triphenylboron and benzene. Triphenylboron subsequently undergoes donor–acceptor adduct formation with the vanadyl complex. The IR spectrum of the complex has a strong peak at 919 cm^{-1}. This is significantly lower than observed in the parent vanadyl complex, 965 cm^{-1}, and is attributed to the weakened V=O–B adduct formation.

Method B

50 mg of $(C_{22}H_{22}N_{22})V{=}O$ were suspended in a solvent mixture of 1:1 toluene: acetonitrile in a test tube. To this suspension, 40 mg of $NaB(C_6H_5)_4$ and 10 mg of *p*-toluenesulfonic acid were added. The rest of the reaction conditions were the same as for method A.

$[(C_{22}H_{22}N_4)V{-}O{-}Si(CH_3)_3]B(C_6H_5)_4$

Fifty mg of $(C_{22}H_{22}N_4)VCl_2.HCl$ or $(C_{22}H_{22}N_4)V{=}O$ were suspended in a solution mixture of 1:1 toluene:acetonitrile in a test tube. To this solution was added 40 mg of sodium tetraphenylboron and 0.3 cm^3 of hexamethyldisilazane, $HN[Si(CH_3)_3]_2$. The test tube was stoppered with a serum cap and kept at room temperature for 12 hours. Dark brown crystals slowly formed. The product was filtered from solution under nitrogen, washed with acetonitrile and dried *in vacuo*. The IR spectrum contained new strong peaks at 903 cm^{-1} and 837 cm^{-1} assigned to the Si–O stretch and CH_3 rocking modes, respectively. A strong peak at 830 cm^{-1} overlapping with one at 837 cm^{-1} was assigned to the V–O stretching frequency.

Crystallographic Data Collection and Refinement of Structures

$(C_{22}H_{22}N)VO$

Crystals of $(C_{22}H_{22}N_4)VO$ were obtained by recrystallization from hot toluene. A saturated solution of the compound in boiling toluene was filtered into a clean test tube. This was stoppered under an inert N_2 atmosphere and immersed in a Dewar flask containing hot (80°C) water. The sample was left standing for 3 days during which time slow cooling of the solution facilitated growth of dark green crystals on the walls of the tube.

TABLE I
Crystallographic data for $VO(C_{22}H_{22}N_4)$ and its adduct complexes.

Formula	$VO(C_{22}H_{22}N_4)$	$VON_4C_{40}BH_{37}$	$VOSiN_4C_{44}BH_{51}$
M. W.	409.45	651.52	801.82
Cryst. Syst.	triclinic	monoclinic	monoclinic
Space Group	$P\bar{1}$	$P2_1/n$	$P2_1/m$
a, Å	11.150(2)	11.174(3)	9.884(1)
b, Å	12.514(3)	20.208(4)	13.669(4)
c, Å	8.468(2)	14.460(8)	16.161(3)
α, deg	101.80(2)	90	90
β, deg	105.09(3)	97.23(1)	105.01(1)
γ, deg	76.27(2)	90	90
V, $Å^3$	1181	3239.1(3.4)	2109
Z	2	4	2
d(*calc*), $g\,cm^{-3}$	1.381	1.336	1.263
d(*obs*), $g\,cm^{-3}$	1.37	1.34	1.28
Crystal Colour	green	brown	brown
Radiation	MoKα	MoKα	MoKα = 0.71073
Diffractometer	Ames	ENRAF-NONIUS CAD-4	
Abs. Coeff., cm^{-1}	5.657	3.328	2.944
Scan Speed	2°/Min	2.2–3.3	4.0
2θ Scan Range	$2 < 2\theta < 50°$	$2 < 2\theta < 50°$	$2 < 2\theta < 55°$
Scan Technique	θ–2θ	θ–2θ	θ–2θ
Data Collected	$h, \pm k, \pm l$	$h, k, \pm l$	$h, k, \pm l$

Examination of the crystals showed that most were twinned. However, a suitable fragment of approximately cubic shape was obtained and mounted on a glass fibre with epoxy resin. Preliminary precession photographs indicated that the compound crystallized in a triclinic space group. Satisfactory refinement assuming a centric model confirmed $P\bar{1}$ as the correct space group. The cell constants for this compound, given in Table I, were determined from the least-squares adjustment of the setting angles from twelve high-angle reflections.

Data were collected at room temperature using a four-circle diffractometer designed and built in the Ames Laboratory (Iowa State University). A scan rate of 0.1 sec/step of 0.01° in θ was employed with a variable scan range of 35 steps plus one step per each degree theta. Within the 2θ sphere of 50°, a total of 4568 reflections were collected. The intensities of five standard reflections were remeasured after every 75 reflections.

The structure was solved using Patterson techniques and refined using full-matrix least-squares methods. In the final cycle, a model assuming anisotropic thermal motions for all nonhydrogen atoms was assumed. All hydrogen atoms were located on a difference Fourier map obtained near the final stages of refinement. The hydrogen atom positions were then calculated assuming idealized geometry with C–H distances of 0.95 Å and 1.00 Å for aromatic and aliphatic C–H hydrogen atoms, respectively. These atoms were included as fixed contributions in the last cycles of least-squares refinement.

The toluene solvent molecule was observed as an extremely diffuse and ill-defined area of electron density in the vicinity of the inversion centre (0.5, 0.5, 0.0). Close inspection of the difference Fourier maps indicated four-fold disorder of the toluene molecule. Since an accurate detailed geometry of the toluene molecule was not of major concern, it appeared that the electron density could best by accounted for by refining the coordinates and anisotropic thermal parameters of the individual atoms of the toluene molecules. The multiplicities of the individual atoms were varied because the methyl groups and the ring carbon atoms were not resolvable due to the nature of the overlap. In the final two cycles of refinement, the conventional R factors converged to $R = 0.054$ and $R_w = 0.072$. The highest peak on the final difference Fourier map had a density of 0.49 e/Å^3, located in the region of the toluene solvent molecule. The final atomic coordinates for the structure are listed in Table II.

$(C_{22}H_{22}N_4)V{=}O{-}B(C_6H_5)_3$

Brown crystals were obtained from the reaction of $(C_{22}H_{22}N_4)VCl_2.HCl$ with $NaB(C_6H_5)_4$ in a solvent mixture of toluene and acetonitrile maintained at 60°C for 12 hours. A good crystal of dimensions 0.40 × 0.40 × 0.10 mm was selected and mounted on a glass fibre. Geometric and intensity data were measured with an Enraf-Nonius CAD4 diffractomer. The unit cell parameters and orientation matrix were refined by a least-squares fit of 25 reflections in the range of $15° < 2\theta < 30°$ using graphite-monochromated MoKα radiation. The systematic absences uniquely determined the space group to be monoclinic, $P2_1/n$. The crystal data, data collection and refinement details are summarized in Table I. Intensity data were collected with θ–2θ scans technique with a scan range of $0.75 + 0.35 \tan\theta$ centred about the calculated MoKα peak position. The scan rate was 2.2–3.3°/min through the data collection. The intensity for each reflection was obtained from $I = F/S[P - 2(B_1 + B_2)]$ where P and B are peak and background count, S is integer inversely proportional to the scan rate and F is either unity or a multiplier to account for the occasional attenuation of the diffraction beam. A total of 6208 independent reflections were measured in the range of $2° < 2\theta < 50°$, and a total of 3678 reflections for which the integrated intensities were higher than 2σ were included. Initial coordinates for non-hydrogen atoms of the complex were obtained from direct methods (MULTAN 78) and difference Fourier maps. Hydrogen atom positions were calculated assuming bond distances of 0.95 Å and isotropic temperature parameters of 5.0. The hydrogen atoms were included, but their parameters were not varied in the

TABLE II
Positional parameters for the atoms of $VO(C_{22}H_{22}N_4)$.

Atom	*x/a*	*y/b*	*z/c*
V	0.15712(4)	0.19875(4)	−0.01527(5)
O	0.2438(2)	0.2447(2)	−0.0994(2)
N1	0.2177(2)	0.2259(2)	0.2334(3)
N2	0.0000(2)	0.3162(2)	0.0081(3)
N3	0.0220(2)	0.1325(2)	−0.1925(3)
N4	0.2442(2)	0.0431(2)	0.0329(3)
C1	−0.0356(3)	0.3725(2)	0.1459(3)
C2	0.0382(3)	0.3573(2)	0.3122(3)
C3	0.1564(3)	0.2892(2)	0.3467(3)
C4	0.3385(3)	0.1569(2)	0.2707(3)
C5	0.4424(3)	0.1862(3)	0.3894(4)
C6	0.5595(3)	0.1147(4)	0.4023(5)
C7	0.5741(3)	0.0152(3)	0.2963(5)
C8	0.4731(3)	−0.0131(3)	0.1745(4)
C9	0.3538(3)	0.0552(2)	0.1607(3)
C10	0.2077(3)	−0.0534(2)	−0.0360(3)
C11	0.0970(3)	−0.0592(2)	−0.1594(3)
C12	0.0087(3)	0.0261(2)	−0.2321(3)
C13	−0.0634(2)	0.2221(2)	−0.2643(3)
C14	−0.1245(3)	0.2205(3)	−0.4309(4)
C15	−0.1971(3)	0.3173(3)	−0.4871(4)
C16	−0.2050(3)	0.4161(3)	−0.3813(4)
C17	−0.1431(3)	0.4208(2)	−0.2158(4)
C18	−0.0742(2)	0.3240(2)	−0.1556(3)
C19	−0.1620(3)	0.4500(3)	0.1410(4)
C20	0.2065(3)	0.2829(3)	0.5297(4)
C21	0.2766(3)	−0.1621(3)	0.0211(5)
C22	−0.1091(3)	−0.0066(2)	−0.3499(4)
C23	0.4952(7)	0.4617(1)	−0.1909(2)
C24	0.4717(2)	0.4036(2)	−0.0018(5)
C26	0.4608(1)	0.3796(1)	0.1875(2)
C27	0.5091(4)	0.4395(3)	−0.2688(6)
C28	0.4736(2)	0.4411(2)	0.1884(4)
C29	0.4699(7)	0.3997(8)	−0.0875(1)
C30	0.4790(7)	0.4390(1)	0.0854(2)

subsequent refinement. The structure was refined by full-matrix least-square techniques. At convergence, the agreement factors were $R = 0.065$ and $R_w = 0.070$. The final difference Fourier maps showed the highest peak of $0.73/e/Å^3$ close to the atoms C12 and C13. The final atomic positional parameters are given in Table III.

$[(C_{22}H_{22}N_4)\ V\text{–}O\text{–}Si(CH_3)_3]B(C_6H_5)_4$

Brown crystals were obtained from the reaction solution containing $(C_{22}H_{22}N_4)VCl_2.HCl$, $HN[Si(CH_3)_3]_2$ and $NaB(C_6H_5)_4$ in a solvent mixture of toluene and acetonitrile at room temperature. After two days, a good crystal of dimensions

TABLE III

Table of positional parameters for atoms of $(C_{22}H_{22}N_4)V{=}O{-}B(C_6H_5)_3$.

Atom	*x/a*	*y/b*	*z/c*
V	0.48959(7)	0.07276(4)	0.72636(5)
O	0.3971(3)	0.0778(2)	0.8078(2)
N1	0.4327(3)	0.1384(2)	0.6279(3)
N2	0.6223(3)	0.1400(2)	0.7446(3)
N3	0.6178(3)	0.0042(2)	0.7552(3)
N4	0.4268(3)	0.0012(2)	0.6390(3)
C1	0.4569(4)	0.2009(2)	0.6691(3)
C2	0.3827(5)	0.2568(3)	0.6604(4)
C5	0.5881(5)	0.2576(3)	0.7902(4)
C6	0.5626(4)	0.2021(2)	0.7351(3)
C7	0.7427(4)	0.1333(3)	0.7601(3)
C7A	0.8277(5)	0.1914(3)	0.7642(4)
C8	0.7953(4)	0.0712(3)	0.7708(3)
C9	0.7386(4)	0.0104(3)	0.7702(3)
C9A	0.8200(5)	−0.0492(3)	0.7817(5)
C10	0.5568(5)	−0.0570(2)	0.7535(4)
C11	0.5832(5)	−0.1089(3)	0.8142(4)
C15	0.4496(4)	−0.0592(2)	0.6883(4)
C14	0.3762(5)	−0.1146(3)	0.6859(4)
C16	0.3699(4)	0.0050(3)	0.5513(3)
C18	0.3787(4)	0.1287(3)	0.5400(3)
C27	0.1759(4)	0.0817(2)	0.7489(3)
C33	0.2633(4)	0.0079(2)	0.9010(3)
C4	0.5143(6)	0.3122(2)	0.7790(4)
C12	0.5105(6)	−0.1649(3)	0.8077(5)
C16A	0.3304(5)	−0.0558(3)	0.4946(4)
C17	0.3495(5)	0.0658(3)	0.5063(3)
C18A	0.3557(6)	0.1846(3)	0.4724(4)
C22	0.1733(6)	0.1471(3)	0.9672(4)
C23	0.1585(7)	0.2019(3)	1.0204(5)
C24	0.2331(7)	0.2553(3)	1.0172(4)
C25	0.3241(6)	0.2517(3)	0.9620(4)
C35	0.1495(6)	−0.0764(3)	0.9729(4)
C36	0.2528(7)	−0.1100(3)	1.0030(4)
C37	0.3605(6)	−0.0867(3)	0.9836(4)
C3	0.4128(6)	0.3121(3)	0.7127(4)
C13	0.4084(6)	−0.1673(3)	0.7441(5)
C26	0.3392(5)	0.1951(3)	0.9092(4)
C28	0.1501(5)	0.1425(3)	0.7060(4)
C29	0.0781(6)	0.1488(3)	0.6211(4)
C30	0.0268(5)	0.0937(3)	0.5768(4)
C31	0.0503(6)	0.0326(3)	0.6170(4)
C32	0.1250(5)	0.0265(3)	0.7016(4)
C34	0.1550(5)	−0.0180(3)	0.9225(4)
C38	0.3659(5)	−0.0284(3)	0.9328(4)
C21	0.2636(4)	0.1414(2)	0.9091(3)
B	0.2702(4)	0.0761(3)	0.8439(4)

$0.40 \times 0.40 \times 0.30$ mm was selected and mounted on a glass fibre. The unit cell constants were obtained by the same method as for the crystal of $(C_{22}H_{22}N_4)V{=}O{-}B(C_6H_5)_3$; the crystallographic data are summarized in Table I. Crystals are monoclinic with systematic absences consistent with either $P2_1$ or $P2_1/m$ space groups. Intensity statistics favoured the centrosymmetric space group $P2_1/m$ and the structure was solved in this space group.

TABLE IV

Positional parameters for the atoms of $[(C_{22}H_{22}N_4)V{=}O{-}Si(CH_3)_3]B(C_6H_5)_4$.

Atom	*x*/*a*	*y*/*b*	*z*/*c*
V	0.55888(8)	0.7500(0)	0.30822(4)
SI	0.3592(1)	0.7500(0)	0.44803(8)
O	0.4312(3)	0.7500(0)	0.3657(2)
N1	0.7077(3)	0.8434(2)	0.3634(1)
N2	0.5129(3)	0.6571(2)	0.2105(1)
C1	0.7670(3)	0.8017(2)	0.4454(2)
C2	0.8052(3)	0.8520(2)	0.5232(2)
C3	0.8477(3)	0.8005(3)	0.5988(2)
C4	0.7495(3)	0.9285(2)	0.3358(2)
C4A	0.8743(4)	0.9834(3)	0.3885(2)
C5	0.6858(4)	0.9664(2)	0.2568(2)
C6	0.5715(3)	0.5739(3)	0.1956(2)
C6A	0.5256(4)	0.5210(3)	0.1110(2)
C7	0.3922(3)	0.6987(3)	0.1544(2)
C8	0.2721(4)	0.6572(4)	0.1108(2)
C9	0.1570(4)	0.6999(4)	0.0662(2)
C11	0.1699(7)	0.7500(0)	0.4089(5)
C12	0.2528(3)	0.3475(2)	0.1904(2)
C13	0.3312(4)	0.4135(3)	0.2499(2)
C14	0.2714(5)	0.4952(3)	0.2791(2)
C15	0.1306(5)	0.5129(3)	0.2497(3)
C16	0.0510(4)	0.4501(3)	0.1925(3)
C17	0.1100(4)	0.3700(3)	0.1634(2)
C18	0.4872(5)	0.2500(0)	0.1768(3)
C19	0.5677(5)	0.2500(0)	0.2618(3)
C20	0.7129(5)	0.2500(0)	0.2846(3)
C22	0.7103(5)	0.2500(0)	0.1380(3)
C23	0.5646(5)	0.2500(0)	0.1165(3)
C25	0.2338(3)	0.3355(3)	−0.0016(2)
C24	0.2554(4)	0.2500(0)	0.0467(2)
C26	0.1945(4)	0.3359(3)	−0.0907(2)
C27	0.1751(6)	0.2500(0)	−0.1352(3)
C21	0.7842(5)	0.2500(0)	0.2221(4)
C10	0.4174(5)	0.6383(3)	0.5116(2)
B	0.3142(5)	0.2500(0)	0.1521(3)

The intensity data were collected by the same method as described for the previous complexes except the scan rate was 4°/min and the scan range was $0.70 + 0.35 \tan\theta$. A total of 5330 independent reflections were measured in the range of $2° < 2\theta < 55°$ and a total of 3597 reflections for which integrated intensities higher than 2σ were used in the solution and refinement of the structure. The coordinates of most non-hydrogen atoms were obtained by the direct methods (MULTAN 78) with the remainder found from difference Fourier maps. The positions of the hydrogens were calculated as for previous structures. Isotropic refinement followed by anisotropic refinement for all non-hydrogen atoms yielded the final agreement factors, $R = 0.058$ and $R_w = 0.069$. The final atomic positional parameters are given in Table IV.

RESULTS AND DISCUSSION

Synthesis and Reactivity

$(C_{22}H_{22}N_4)V{=}O$

The reaction of vanadyl acetate with the free ligand $C_{22}H_{24}N_4$ in toluene, under nitrogen, affords a yellow-green crystalline material, with elemental analyses corresponding to $(C_{22}H_{22}N_4)VO$. The mass spectrum of this solid exhibited a peak at an m/e value corresponding to a molecular weight of $(C_{22}H_{22}N_4)V{=}O$. The IR spectrum contains a band at 965 cm^{-1} assignable to the V=O stretching frequency. This is approximately 30–35 cm^{-1} lower than vanadyl acetylacetones, porphyrins and phthalocyanines (Table V) and probably reflects a slightly weaker V=O bond strength. This is an important factor in the enhanced reactivity of the V=O group of this complex compared to other vanadyl complexes. The compound is soluble in chloroform and moderately soluble in acetonitrile and toluene.

The electronic spectra exhibit the usual d–d transitions expected for V(IV) in a strong tetragonal field. The three absorbtions are assigned as follows, $B_{2g} \rightarrow E_g$, 736.2 nm (13.58 kK); $B_{2g} \rightarrow E_{1g}$, 414.8 nm (24.12 kK); and $B_{2g} \rightarrow A_{1g}$, 376.7 nm (26.55 kK) (partially obscured by metal–ligand and ligand–ligand charge transfer absorbtions).

$(C_{22}H_{22}N_4)V{=}O$ is deoxygenated by reaction with anhydrous HCl to form a compound of composition $(C_{22}H_{22}N_4)VCl_2.HCl$. The IR spectrum is devoid of any absorbtions assignable to the V=O group and contains multiple absorbtions in the 1600–1500 cm^{-1} region attributable to both delocalized β-2,4-pentanediiminato chelate rings, as well as isolated imine functions which are produced on protonation of the γ–C atom of these rings. Similar IR spectra have been observed with other monoprotonated species $Ni(C_{22}H_{22}N_4)$. $HClO_4$, for which NMR studies corroborate the site of ligand protonation. Insolubility of the complex in chloroform and toluene are consistent with an ionic formulation. $(C_{22}H_{22}N_4)VCl_2.HCl$ decomposes immediately to $(C_{22}H_{22}N_4)V{=}O$ in the presence of trace amounts of water. Attempts to deprotonate resulted in hydrolysis to $(C_{22}H_{22}N_4)V{=}O$. It is believed that the structure of the complex is similar to the six-coordinate complex *cis*-dichloro $(C_{22}H_{22}N_4)TiCl_2$.[9] Although the structure is unknown, this material serves as a convenient starting material for V(IV) complexes of this ligand other than those containing vanadyl alone.

The reaction of $(C_{22}H_{22}N_4)V{=}O$ with $NaB(C_6H_5)_4$ in a solvent mixture of toluene and acetonitrile under acidic conditions yields $(C_{22}H_{22}N_4)V{=}O{-}B(C_6H_5)_3$. The IR spectrum contains a strong absorbtion at 919 cm^{-1} assignable to the V=O stretching frequency. This 46 cm^{-1} lowering from the "free" vanadyl complex is attributable to bond weakening due to V=O–B adduct formation.

The sequence of reactions leading to this product is believed to be as follows.

$NaB(C_6H_5)_4$ reacts with acid yielding $B(C_6H_5)_3$, an oxophilic species, which subsequently reacts with $(C_{22}H_{22}N_4)V{=}O$ forming the adduct $(C_{22}H_{22}N_4)V{=}O{-}B(C_6H_5)_3$. The same adduct is obtained by reaction with $NaB(C_6H_5)_4$ with $(C_{22}H_{22}N_4)VCl_2.HCl$ in solvents with a trace of water. $(C_{22}H_{22}N_4)VCl_2.HCl$ liberates "free" HCl, which then serves the same purpose as the acid described in the synthesis. Crystalline $(C_{22}H_{22}N_4)V{=}O{-}B(C_6H_5)_3$ is air-stable for months. When suspended in acetonitrile solution, it decomposes gradually to $(C_{22}H_{22}N_4)V{=}O$. The compound does not dissolve in either polar or non-polar solvents. It reacts with HCl to yield $(C_{22}H_{22}N_4)VCl_2.HCl$, and with $HN[Si(CH_3)_3]_2$ to yield $[(C_{22}H_{22}N_4)V{-}O{-}Si(CH_3)_3]^+$ (apparently from oxo impurities in $HN[Si(CH_3)_3]_2$).

$[(C_{22}H_{22}N_4)V{-}O{-}Si(CH_3)_3]B(C_6H_5)_4$ was obtained from the reaction of $HN[Si(CH_3)_3]_2$ either with $(C_{22}H_{22}N_4)V{=}O$ or with $(C_{22}H_{22}N_4)VCl_2.HCl$ and was crystallized by adding anions such as $B(C_6H_5)_4^-$. The compound is air-stable in the solid state. When the compound is dissolved in acetonitrile, the solution changes from brown to green in colour. The green coloured product has been isolated and proven to be a dimer, which is also obtained from the reaction of $(C_{22}H_{22}N_4)V{=}O$ with oxidizing reagents such as oxygen or H_2O_2 when anions such as PF_6^-, or $B(C_6H_5)_4^-$ are present.

Crystal Structures

$(C_{22}H_{22}N_4)V{=}O$

The structure of $(C_{22}H_{22}N_4)V{=}O$ consists of a molecular five coordinate oxovanadium complex in which the planar coordination environment is provided by the macrocycle ligand $C_{22}H_{22}N_4^{2-}$. A side view of the molecule and the atom labelling scheme in Figure 1 illustrates the saddle-like shape of the ligand and its inner coordination sphere. The interatomic bond distances and angles of the coordination sphere are given in Table V. The V(IV) is displaced 0.673 Å from the N_4 coordination plan toward the oxygen atom. The macrocycle has assumed a saddle-shaped conformation due primarily to steric interactions of the benzenoid ring with the methyl groups attached to the delocalized 6-membered ring. The V=O bond length of 1.601(2) Å is not significantly different from those of the porphyrin or phthalocyanine complexes vanadyl octaethylporphyrin[10] (1.620 Å), vanadyl deoxophylloerythro-ethioporphyrin[11] (1.619 Å) and oxovanadium(IV) phthalocyanine[12] (1.580 Å).

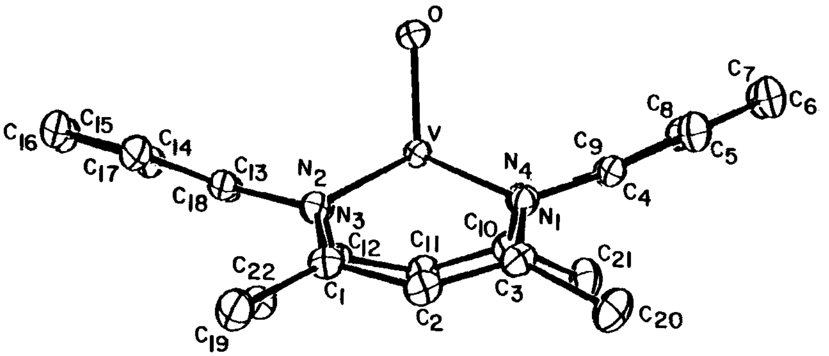

FIGURE 1 Side view of $VO(C_{22}H_{22}N_4)$ illustrating the double saddle shape of the ligand and elevation of V from the N_4 coordination plane. Thermal ellipsoids are drawn at the 50% probability level.

TABLE V

Interatomic bond distances and angles for the coordination sphere of $VO(C_{22}H_{22}N_4)$.

(a)	*Distances (Å)*	*(b)*	*Angles (°)*
V–O	1.601(2)	O–V–N1	109.6(1)
V–N1	2.020(2)	O–V–N2	109.3(1)
V–N2	2.026(2)	O–V–N3	109.9(1)
V–N3	2.028(2)	O–V–N4	108.7(1)
V–N4	2.031(2)	N1–V–N2	88.5(1)
		N1–V–N3	140.5(1)
		N1–V–N4	78.4(1)
		N2–V–N3	78.5(1)
		N2–V–N4	141.9(1)
		N3–V–N4	89.2(1)

The $V{=}O^{2+}$ bond strenth and consequently the V=O distance is influenced by the pπ-donor properties of the equatorial ligands. Comparison of the values listed in Table VI reveals that the V=O distance generally decreases as the in-plane ligand field decreases except for the phthalocyanine ligand. The ligand fields increase according to the series acac < acen < $C_{22}H_{22}N_4^{2-}$ < OEP < PC and the V=O bond distance increases in the same order.

TABLE VI

Comparison of the structural parameters of related vanadyl complexes.

Compound	V=O Bond Distance (Å)	V–N Bond Distance (Å)	Displacement of V from N_4 (Å)	V= IR Spectra (cm^{-1})	Ref.
$(C_{22}H_{22}N_4)V{=}O$	1.601(2)	2.026(2)	0.673	965	[a]
$(C_{22}H_{22}N_4)V{=}O{-}BPh_3$	1.665(3)	1.994(3)	0.667	919	[a]
$[(C_{22}H_{22}N_4)V{-}O{-}Si(CH_3)_3]B(C_6H_5)_4$	1.751(3)	1.982(3)	0.684	830	[a]
VO(DPEP)	1.619(7)	2.10(1)	0.48	1001	11
VO(OEP)	1.620(2)	2.102(6)	0.543	1000	10
VO(PC)	1.580(3)	2.026(7)	0.575	990	12
VO(acen)	1.585(7)	2.053(9)	0.58	982	13
VO(acac)	1.56(1)		0.548	995	14

[a] This work.

The displacement of the V atom from the N_4 coordination plane of previously reported regular square pyramidal vanadyl complexes ranges from 0.537 Å in VO(DPEP)[11] to 0.58 Å in VO(acen).[13] The displacement of 0.673 Å observed in $(C_{22}H_{22}N_4)V{=}O$ is significantly greater. The increased displacement of the vanadium from the N_4 plane is accompanied by tortional motions about the appropriate bonds to direct the lone pairs out of the N_4 plane thus reducing overlap with the vanadium $d_{x^2-y^2}$ orbital. Simultaneously, the nitrogen lone pairs are directed more towards the unfilled d_{xz} and d_{yz} orbitals of vanadium which also participate in π bonding with oxygen and now compete with it. This competitive interaction may be responsible for some weakening of the V=O bond strength as indicated by the 30 to 36 cm^{-1} decrease in the V=O stretching frequency.

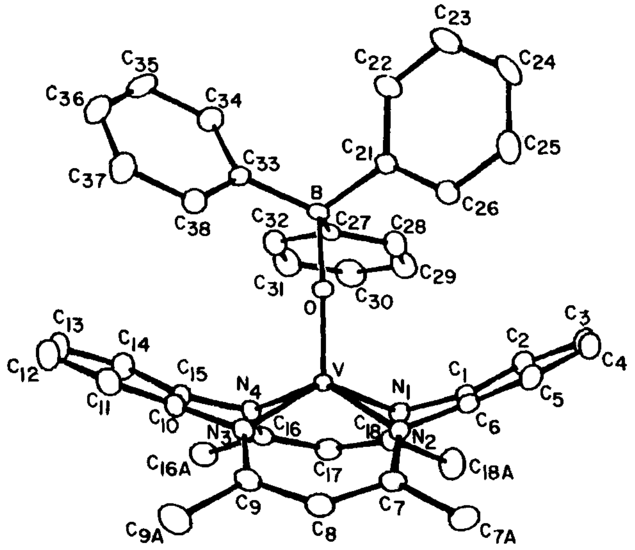

FIGURE 2 Side view and labelling scheme of $(C_{22}H_{22}N_4)V\text{-}O\text{-}B(C_6H_6)_3$ illustrating the V-O-B linkage.

$(C_{22}H_{22}N_4)V{=}OB(C_6H_5)_3$

This structure consists of the molecular five-coordinate donor-acceptor complex between $(C_{22}H_{22}N_4)V{=}O$ and $B(C_6H_5)_3$. Figure 2 contains the labelling scheme with a view of the molecule from the side. The vanadium is bound to four nitrogen atoms of the macrocyclic ligand and an oxygen atom which has formed an adduct with $B(C_6H_5)_3$. Table VII lists the more important bond distances and bond angles for this structure. The V=O bond distance, 1.665(3) Å, is lengthened only slightly; 0.064 Å from the adduct free complex, 1.601 Å. This modest increase is surprising given the normal avidity of B for oxygen donors. The V displacement, 0.677 Å, from the N_4 coordination plane toward the oxygen atom is unchanged from that of the "free" complex. The average V–N bond distance, 1.994(3) Å, is only marginally shorter than that of $(C_{22}H_{22}N_4)V{=}O$, 2.026(2) Å. The V–O–B bond angle is 154.1(2)°. The B–O bond distance, 1.571(5) Å, is significantly longer than normal B–O single bonds, 1.36Å.[15] The average B–C bond distance, 1.623(6) Å, is nominally shorter than observed in the $B(C_6H_5)_4^-$ ion of $[(C_{22}H_{22}N_4)V\text{–}O\text{–}Si(CH_3)_3]B(C_6H_5)_4$, 1.653(5) Å, a reflection of the electron deficit resulting from the weak B–O bond. The noticeable flattening of the $B(C_6H_5)_3$ group as indicated by an increase of the C–B–C bond angles from tetrahedral to 113.0(4)° in $(C_{22}H_{22}N_4)V{=}O\text{–}B(C_6H_5)_3$ reflects the same phenomena.

$[(C_{22}H_{22}N_4)V\text{–}O\text{–}Si(CH_3)_3]B(C_6H_5)_4$

The structure of this compound consists of a cationic $(C_{22}H_{22}N_4)V\text{–}O\text{–}Si(CH_3)_3^+$ unit with a $B(C_6H_5)_4^-$ anion. Figure 3 provides a side view of $[(C_{22}H_{22}N_4)V\text{–}O\text{–}Si(CH_3)_3^+$ together with the labelling scheme. Important bond distances and bond angles are summarized in Table VIII. The structure consists of a five-coordinate

TABLE VII

Bond distances and angles for the coordination sphere of $(C_{22}H_{22}N_4)V{=}O{-}B(C_6H_5)_3$.

(a)	*Distances (Å)*	*(b)*	*Angles (°)*
V-N1	1.990(4)	N1-V-N2	78.8(2)
V-N2	2.005(4)	N1-V-N3	140.1(2)
V-N3	1.999(4)	N1-V-N4	88.6(2)
V-N4	1.984(4)	N2-V-N3	86.8(2)
V-O	1.665(3)	N2-V-N4	140.6(2)
O-B	1.571(6)	N3-V-N4	79.3(2)
		N1-V-O	107.1(2)
		N2-V-O	112.3(2)
		N3-V-O	112.8(2)
		N4-V-O	107.0(2)
		V-O-B	154.1(4)

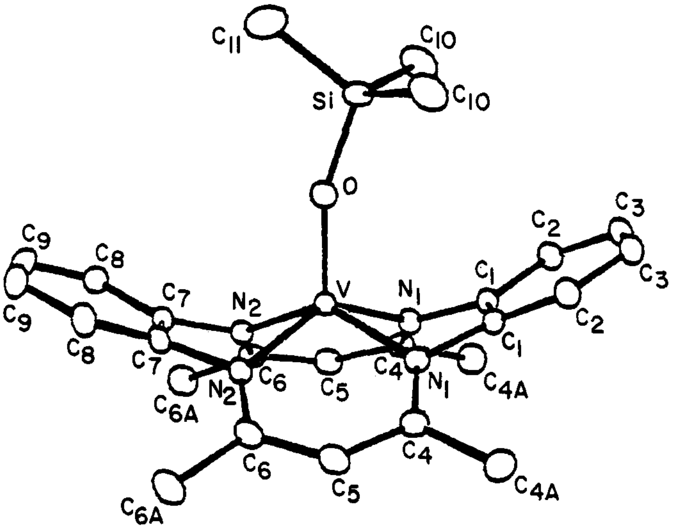

FIGURE 3 Side view of the $[C_{22}H_{22}N_4)VO{-}Si(CH_3)_3]^+$ cation, with labelling scheme, illustrating the displacement of the V atom from the N_4 plane toward the oxygen atom.

vanadium macrocyclic complex with the metal ion bound to four nitrogen atoms of the macrocycle and one oxygen atom which also bridges the V and a trimethylsilyl group. The V–O bond distance, 1.751(3) Å, is lengthened substantially from the free VO distance of the aforedescribed boron adduct. The vanadium is displaced 0.682 Å from the N_4 coordination plane toward the oxygen atom. The average V–N bond distance, 1.982(3) Å, is only slightly shorter than that of the related compounds, $(C_{22}H_{22}N_4)V{=}O$, $(C_{22}H_{22}N_4)V{=}O{-}B(C_6H_5)_3$ and other vanadyl porphyrin compounds.[10,12] The bond length of V–O is longer than of typical vanadyl complexes (1.56–1.62 Å), but shorter than the μ-oxo bridge of homobinuclear dimer complexes (V–O 1.80 Å).[16] The V–O–Si bond angle is 160.3(1)°; there does not appear to be any obvious correlation between M–O–Si linkages and bond lengths (see Table IX). The bond lengths of Si–O and Si–C are 1.662(3) Å and 1.872(7) Å respectively. The silicon is bound to three methyl carbons and an oxygen atom with an average C–Si–C angle of 110.5(5)°.

TABLE VIII

Bond distances and angles for the coordination sphere of the $(C_{22}H_{22}N_4)V{=}O{-}Si(CH_3)_3{}^+$ cation.

(a)	*Distances (Å)*	*(b)*	*Angles (°)*
V–O	1.751(3)	N1–V–N1	80.4(1)
O–Si	1.662(3)	N1–V–N2	86.4(1)
V–N1	1.978(3)	N1–V–N2	139.6(1)
V–N2	1.986(3)	N2–V–N2	79.4(1)
		O–V–N2	112.0(1)
		O–V–N1	108.4(1)
		V–O–Si	160.3(1)

Table IX compares the structural parameters for the V–O–Si compound with those of related trimethylsiloxy metal complexes. The Si–O distance, 1.662(3) Å, in $[(C_{22}H_{22}N_4)V{-}O{-}Si(CH_3)_3]^+$ is the longest among related compounds containing Si–O linkages. These bond parameters provide some indication of the unequal competition of Si and V for the oxo group with the V(IV) clearly having the more effective bonding interaction. The bond distances of O–Si and V–O in $[(CH_3)_3SiO]_3V{=}N$(1-adamantyl) are 1.615(2) Å and 1.763(2) Å, respectively.[19] Obviously, the Si–O bond interactions in this compound are much stonger than in $[(C_{22}H_{22}N_4)V{-}O{-}Si(CH_3)_3]^+$. However, with three V–O bonds, each competing to some extent for π-bonding, the V–O interactions are expected to be weaker because of the competition for metal π-bonding orbitals of the three oxygen atoms around vanadium but will be greater than with a single V–O–Si linkage, as in our adduct.

TABLE IX

Comparison of structural parameters of related trimethylsiloxyl metal complexes.

Compound	M–O–Si Bond Angles (°)	O–Si Bond Distance (Å)	M–O Bond Distance (Å)	Ref.
$[(C_{22}H_{22}N_4)V{-}O{-}Si(CH_3)_3]$ $B(C_6H_5)_4$	160.3(1)	1.662(2)	1.751(3)	[a]
$[(CH_3)_3Si]_2O$	148.0(3)	1.631(3)	1.631(3)	17
(salen)$Fe{-}O{-}Si(CH_3)_3$	142.7(4)	1.633(6)	1.834(6)	18
$(C_{22}H_{22}N_4)Ti[OSi(CH_3)_3]_2$	166.7(8)	1.60(1)	1.84(1)	[b]
$(Me_3SiO)_3V{=}N$(1-adamantyl)	148.7(1)	1.612(2)	1.762(2)	19
	152.7(1)	1.621(2)	1.765(2)	
	154.1(1)	1.615(2)	1.762(2)	

[a] This work. [b] Unpublished data.

TABLE X

Spin Hamiltonian parameters for selected vanadyl complexes.

	LV=O	LV=O–B(C_6H_5)$_3$	LV–O–Si(CH_3)$_3^+$	VO(TPP)	VO(PC)	(CY)(AC)VOPF$_6$	(ACEN)V=O	(ACAC)V=O
g	1.9786	1.9782		1.980	1.980	1.9664	1.974	1.969
g_z	1.9596	1.9702		1.966	1.968	1.954	1.954	1.945
$g_{x,y}$	1.9822	1.9882		1.987	1.987	1.9797	1.984	1.980
a	94.7G	83.9G		97.0G	99.5G	99.0G	102.2G	106.0G
a_z	161.4G	139.0G		173G	174.4G	175.2G	182.0G	188.0G
$a_{x,y}$	61.4G	56.4G		59G	62G	61.0G	62G	65G
g_o	1.9790	1.9730	1.9649			1.9797		
a_o	88.57G	70.34G	62.80G			97.89G		
P	312.78	286.94		355.64	351.54	350.0	369.0	374.0
V=O Distance (Å)	1.601	1.665	1.751	1.620	1.580	1.585	1.580	1.560
Solv.	CH_3CN/tol	CH_3CN/tol	CH_3CN/tol	$CHCl_3$	H_2SO_4	CH_3CN/DMF	THF	THF
Ref	[a]	[a]	[a]	22	21	23	22	22

[a] This work, L = $C_{22}H_{22}N_4^{2-}$; TPP: tetraphenylporphyrin, PC: phthalocyanine.

Comparison of the Structures of the Three Complexes

Some bond parameters for the compounds $(C_{22}H_{22}N_4)V{=}O$, $(C_{22}H_{22}N_4)V{=}O{-}B(C_6H_5)_3$, $[(C_{22}H_{22}N_4)V{-}O{-}Si(CH_3)_3]B(C_6H_5)_4$ and other related vanadyl compounds are summarized in Table VII. Comparison of the three structures reveals the following trends. The bond distance of V–O increases from 1.601 Å for the simple vanadyl complex to 1.751 Å for the trimethylsilyl adduct and follows the expected trends, increasing with increasing adduct strength. The V–N bond distance decreases from 2.062 Å for the vanadyl to 1.982 Å for the silyl complex, reflecting the tighter V–N bonding as the V=O bond weakens. The distance of the metal from the N_4 plane is virtually invariant among the three complexes. Finally, the Ct–N distance decreases from 1.912 Å for the vanadyl to 1.860 Å for that of the silyl derivative, also reflecting the tighter V–N bonding with decreasing V=O interaction.

EPR Spectra

The vanadyl ion, with one unpaired electron, is easily detected by EPR techniques and provides a tool to test conclusions drawn from our structural studies. The isotropic EPR spectral parameters for g_0 and a_0 as well as the principal components of the $<g>$ tensor and the hyperfine interaction $<a>$ for $(C_{22}H_{22}N_4)V{=}O$, $(C_{22}H_{22}N_4)V{=}O{-}B(C_6H_5)_3$, $[(C_{22}H_{22}N_4)V{-}O{-}Si(CH_3)_3]B(C_6H_5)_4$ and related vanadyl compounds are presented in Table X. The spectra are characteristic of a d^1, $I = 7/2$, V^{+4} ion in a tetragonally distorted environment.

Although the molecular symmetry of the compounds is actually C_{2v} rather than C_{4v}, a rhombic distortion was not observed in the spectra. Apparently the very strong V=O bonding desensitizes the involved orbitals to the weaker interactions from the four nitrogen atoms of the macrocyclic ligand. Nitrogen superhyperfine structure was not observed although it can be seen in the spectra of closely related vanadyl porphyrins and phthalocyanine complexes at room temperature. In the latter complexes, the amount of electron density delocalized into the nitrogen ligand is less than 5%, and typical A^N values are of the order of 2–5%. However, for the ground state of $(C_{22}H_{22}N_4)V{=}O$, the unpaired electron is almost totally localized in the d_{xy} orbital.

The variation of charge on the vanadium ion for the different compounds can be obtained from analysis of the EPR spectra. The value of P, where $P = g_eB_eg_N<r^{-3}>$, is proportional to $<r^{-3}>$.[5] A decrease in P implies an increase in the radial extension of the $3d_{xy}$ orbital, the residency of the unpaired electron, and consequently, a decrease on the charge of the metal. The calculated P values for various compounds are listed in Table X. The values of P were obtained using the equation[22]

$$A_z - A_{xy} = -P[6/7(B_2{}^*)^2 + g_z - 5/14\, g_{x,y}$$

where $(\beta_2{}^*)^2 = 1$, $g_z = g_e - g_z$, $g_{xy} = g_e - g_{x,y}$.

From Table X it can be seen that $(C_{22}H_{22}N_4)V{=}O$ and its adduct derivatives have smaller P values than other vanadyl compounds. This implies that $(C_{22}H_{22}N_4)V{=}O$ has a lower charge on the metal, consistent with the strong σ-donor properties of the dianionic ligand, and decreased V=O bond strength as deduced from IR and X-ray structural results. $VO(acac)_2$ has the highest charge on vanadium, consistent with its weaker O_4 donor set as compared to N_4 ligand donor sets. Although both VO(TPP) and VO(PC) contain N_4 donor ligands, large P values are observed. Because of the aromatic framework of these ligands, the N atoms are not as basic as those of $C_{22}H_{22}N_4{}^{2-}$ and the π-acceptor properties of these ligands both contribute to an increase of charge on the vanadium. The small P value (low charge on vanadium) of $(C_{22}H_{22}N_4)V{=}O{-}B(C_6H_5)_3$ can be accounted for by the increased in-plane field strengths as indicated by the decreased V–N distances on vanadyl adduct formation.

The difference of the g_z from free electron value, g_e, is inversely related to the splitting between the $d_{x^2-y^2}$ and d_{xy} levels. Strong ligand fields raise the $d_{x^2-y^2}$ level and lead to an increase in g_z. The correlation between g_z, the V–N (or V–O, planar) and V=O distances are as predicted. The values of g_z increase in the following order for $(C_{22}H_{22}N_4){=}O$ and its related complexes: VO(acac), 1.944 < VO(acen), 1.954, = cis $[VO(CYCLAM)AC]PF_6$, 1.954 < $VO(C_{22}H_{22}N_4)$, 1.9596 < VO(TPP), 1.966, < VO(PC), 1.968 < $(C_{22}H_{22}N_4)V{=}O{-}B(C_6H_5)_3$, 1.9702. Note that the complexes of weaker ligands have lower g_z values; g_z increases with increasing ligand field strength and correlates with the V=O bond distance (with the exception of VOPC).

The anisotropic g value, $g = g_z - g_{xy}$, should be a function of the difference in the axial and in-plane ligand field.[23] Accordingly $(C_{22}H_{22}N_4)V{=}O{-}B(C_6H_5)_3$ has the smallest value, 0.012, because it has the weakest V=O and strongest V–N interactions based on bond length considerations. VO(PC) also has a small g value, 0.019, because of the short V–N distances and consequent strong planar field of the phthalocyanine ligand.

The EPR spectrum of $[(C_{22}H_{22}N_4)V{-}O{-}Si(CH_3)_3]^+$ in a solvent mixture of acetonitrile and toluene was observed at room temperature but no signal was observed in the frozen solution at −140°. A possible reason for losing the EPR signal at low temperature is dimerization of the type illustrated below.

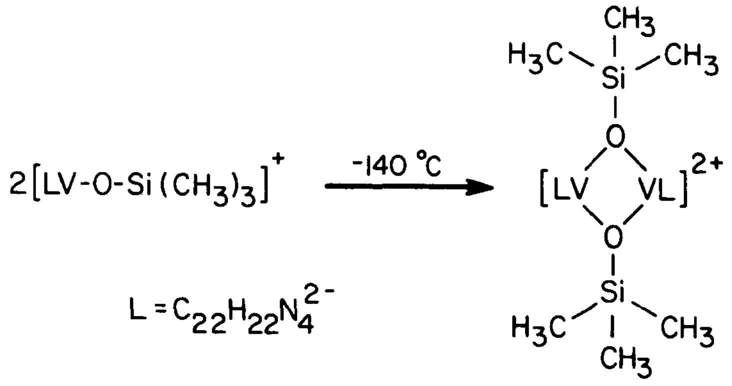

The room temperature EPR spectrum of this compound has the smallest isotropic g value and the smallest isotropic hyperfine constant, 62.8 G, compared with the compounds $(C_{22}H_{22}N_4)V{=}O$ and $(C_{22}H_{22}N_4)V{=}O{-}B(C_6H_5)_3$. The small hyperfine constant indicates a low positive charge on the vanadium; this is consistent with the increased negative charge placed on vanadium by the shortening of the V–N distances upon adduct formation with silicon. Although the g_z value could not be measured, from the weak bonding in V=O a small energy splitting between $d_{x^2-y^2}$ and d_{xy} is predicted.

ACKNOWLEDGEMENTS

The financial support of ACA-PRF is appreciated. We thank Professor Ronald Jacobson of Iowa State University for the use of his diffractometer for the data collection for $VO(C_{22}H_{22}N_4)$.

SUPPLEMENTARY MATERIAL AVAILABLE

A complete set of distances and angles for $VO(C_{22}H_{22}N_4)$ (Table XI), a complete set of distances and angles for $(C_{22}H_{22}N_4)V{-}O{-}B(C_6H_5)_3$ (Table XII), a complete set of distances and angles for $[C_{22}H_{22}N_4)Si{-}O{-}Si(CH_3)_3]B(C_6H_5)_4$ (Table XIII), hydrogen atom coordinates for $(C_{22}H_{22}N_4)V{-}O{-}B(C_6H_5)_3$ (Table XIV), hydrogen atom coordinates for $[(C_{22}H_{22}N_4)V{-}O{-}Si(CH_3)_3]B(C_6H_5)_4$, (Table XV), anisotropic thermal parameters for $VO(C_{22}H_{22}N_4)$ (Table XVI), anisotropic thermal parameters for $(C_{22}H_{22}N_4)V{-}O{-}B(C_6H_5)_3$ (Table XVII), anisotropic thermal parameters for $[(C_{22}H_{22}N_4)V{-}O{-}Si(CH_3)_3]B(C_6H_5)_4$. (Table XVIII), F_{obs} *vs* F_{calc} data for $VO(C_{22}H_{22}N_4)$ Table XIX, (19 pages), F_{obs} *vs* F_{calc} data for $VO(C_{22}H_{22}N_4)V{-}O{-}B(C_6H_5)_3$ Table XX (16 pages), lists of F_{obs} *vs* F_{calc} for $[C_{22}H_{22}N_4)V{-}O{-}Si(CH_3)_3]B(C_6H_5)_4$ Table XXI, (16 pages) are available from the Editor.

REFERENCES

1. R.K. Murmann, *Inorg. Chim. Acta*, **25**, L43 (1977).
2. J. Berkowitz, W.A. Chupka and M.G. Inghram, *J. Chem. Phys.*, **27**, 87 (1957).
3. M. Pasquali, A. Torres-Filho and C. Floriani, *Chem. Comm.*, 534 (1975).
4. M. Pasquali, F. Marchetti and C. Floriani, *Inorg. Chem*, **18**, 2401 (1979).
5. K.P. Callahan and P.J. Durand, *Inorg. Chem.*, **19**, 3211 (1980).
6. K.P. Callahan, P.J. Durand and P.H. Riegen, *Chem. Comm.*, 75 (1980).
7. H.D. Smeidt, A. Persoons and L.D. Maeyer, *Inorg. Chem.*, **13**, 90 (1974).
8. V.L. Goedken and J.A. Ladd, *Chem. Comm.*, 910 (1981).
9. V.L. Goedken and J.A. Ladd, *Chem. Comm.*, 142 (1982).
10. F.S. Molinnaro and J.A. Ibers, *Inorg. Chem.*, **15**, 2278 (1976).
11. R.C. Petterson, *Acta Cryst.*, **B25**, 2527 (1969).
12. R.F. Ziolo, C.H. Griffiths and J.M. Troup, *J. Chem. Soc., Dalton Trans.*, 2301 (1980).
13. D. Bruins and D.L. Weaver, *Inorg. Chem.*, **9**, 130 (1970).
14. R.R. Dodge, D.H. Templeton and A. Zalkin, *J. Chem. Phys.*, **35**, 55 (1961).
15. (a) W.H. Zachariasen, *Acta Cryst.*, **2**, 305 (1954), (b) S.V. Berger, *Acta Cryst.*, **5**, 389 (1952).
16. K. Wieghardt, W. Hulzbach and J. Weiss, *Inorg. Chem.*, **20**, 3436 (1981).
17. B. Csakvari, Z.W. Gomory, F.C. Mijlhoff, B. Rozsonda and I. Hargittai, *J. Organometal. Chem.*, **107**, 287 (1976).
18. S.J. Dzugan and V.L. Goedken, *Inorg. Chim. Acta*, **119**, 43 (1986).
19. W.A. Nugent and R.L. Harlow, *Chem. Comm.*, 342 (1979).
20. M. Sato and T. Kwan, *Bull. Chem. Soc. Jpn.*, **47**, 1353 (1974).
21. M. Sato and T. Kwan, *J. Chem. Phys.*, **50**, 558 (1969).
22. M. Iannuzzi and P.H. Rieger, *Inorg. Chem.*, **14**, 2895 (1975).
23. L.J. Boucher, E.C. Tynan and T.F. Yen, in *ESR of Metal Complexes*, T.F. Yen Ed. (Plenum Press, New York, 1968).